ChemSystemsChem

Research Article
doi.org/10.1002/syst.202400056

Chemistry Europe
European Chemical Societies Publishing

www.chemsystemschem.org

Phase-Separated Droplets Can Direct the Kinetics of Chemical Reactions Including Polymerization, Self-Replication and Oscillating Networks

Iris B. A. Smokers[+],[a] Brent S. Visser[+],[a] Wojciech P. Lipiński,[a] Karina K. Nakashima,[a, b] and Evan Spruijt*[a]

Phase-separated compartments can localize (bio)chemical reactions and influence their kinetics. They are believed to play an important role both in extant life in the form of biomolecular condensates and at the origins of life as coacervate protocells. However, experimentally testing the influence of coacervates on different reactions is challenging and time-consuming. We therefore use a numerical model to explore the effect of phase-separated droplets on the kinetics and outcome of different chemical reaction systems, where we vary the coacervate volume and partitioning of reactants. We find that the rate of bimolecular reactions has an optimal dilute/coacervate phase volume ratio for a given reactant partitioning. Furthermore, coacervates can accelerate polymerization and self-replication reactions and lead to formation of longer polymers. Lastly, we find that coacervates can 'rescue' oscillating reaction networks in concentration regimes where sustained oscillations do not occur in a single-phase system. Our results indicate that coacervates can direct the outcome of a wide range of reactions and impact fundamental aspects such as yield, reaction pathway selection, product length and emergent functions. This may have far-reaching implications for origins of life, synthetic cells and the fate and function of biological condensates.

Introduction

It is hypothesized that phase-separated droplets called coacervates play important roles both in extant life and at the origins of life.[1–4] Cellular coacervates are commonly called membraneless organelles or biomolecular condensates and they include the nucleolus, stress granules and Cajal bodies.[5] Their functions in health include cellular organization, signaling and RNA processing, but emerging evidence suggests that coacervates also play a role in protein aggregation, linking them to neurodegenerative diseases.[6,7] In the origins of life field, coacervates have been proposed as protocells: a first generation of cellular compartments in which processes important to proto-life could be localized.[3,4,8]

In all these cases, the local physicochemical milieu inside the coacervate or biomolecular condensate offers a distinct environment that can significantly influence (bio)chemical reactions. Guest molecules that have favorable interaction with the coacervate components are locally enriched inside the droplets, while molecules that do not interact are excluded. At equilibrium, a constant ratio of concentrations is maintained between the dense coacervate phase and the dilute surrounding phase, which is governed by the partition coefficient K_P, while at the same time molecules are continuously exchanged between the coacervate and its surroundings. This enhanced local concentration and exchange has been shown to affect the kinetics of reactions in coacervates.[9–17] Additionally, the local polarity, crowding, pH and water activity can have substantial effects on the energy landscape of reactions, affecting both reaction rates and pathways.[4,18]

A wide range of reactions have been shown to be enhanced by localization to a coacervate, including enzymatic[9,13,15–17,19] and nanoparticle-catalyzed[9,20] reactions, ribozyme reactions,[14,21–23] reactions between synthetic and prebiotically-relevant small molecules,[10–12,24,25] template-directed RNA polymerization,[26] DNA ligation[27] and cell-free gene expression.[28] Our group has recently also shown that coacervates can lead to preferential formation of specific products in peptide ligation by oxidative coupling of α-amidothioacids and amino acids,[25] showcasing that coacervates can not only accelerate reactions, but also direct reaction pathways. We hypothesize that coacervates can have significant and non-trivial effects on a range of reaction types and in reaction networks. However, experimentally testing these effects is challenging and time-consuming. Computer model predictions may provide a solution to identify interesting reaction types and elucidate design principles for desired reaction outcomes, and can serve as a guide for experiments. Previous theoretical work has provided fundamental insights into processes such as

[a] Institute for Molecules and Materials, Radboud University, AJ Nijmegen, The Netherlands
[b] Institut de Science et d'Ingénierie Supramoléculaires (ISIS), CNRS UMR 7006, Université de Strasbourg, Strasbourg, France

Correspondence: Dr. Evan Spruijt, Institute for Molecules and Materials, Radboud University, Heyendaalseweg 135, 6523 AJ Nijmegen, The Netherlands.
Email: e.spruijt@science.ru.nl

[+] These authors contributed equally to this work

Supporting Information for this article is available on the WWW under https://doi.org/10.1002/syst.202400056

protein aggregation,[29,30] heterodimerization and cluster formation,[31] and enzymatic activity in coacervates,[32] but a versatile and easily adaptable model for practical chemical reactions and reaction networks that is able to explain how experimental systems can be optimized to get a desired reaction outcome, is still lacking.

In this work we use a numerical model to investigate how coacervates can affect the kinetics of reactions that are relevant for (the emergence of) life, based on changes in the partition coefficient of reagents and products, local changes in rate constant and exchange between the dense and dilute phase. We find that the rate of elementary reactions in coacervates can be optimized by tuning the partition coefficient and volume ratio between the dilute and coacervate phase. Polymerization and self-replication reactions can be accelerated in a two-phase system, and coacervates can favor the formation of longer polymers, while locally improving polydispersity, possibly allowing for better information storage in coacervate protocells. Lastly, we find that for oscillating reaction networks the periodicity and amplitude of oscillations can be altered by incorporation in a two-phase system, and oscillations can even be 'rescued' in concentration regimes where sustained oscillations do not take place in a single-phase system.

Results and Discussion

Numerical Model Description

In all systems presented in this paper we assume that reactions occur in a two-phase system, composed of two compartments representing the dilute phase and the dense phase of a physical phase-separated system. We consider reactants and products to be dilute guest molecules that are not involved in phase separation and that exhibit ideal solution behavior. We assume that the reactants do not change the volume, viscosity, density or polarity of the dense phase upon partitioning, so their reaction rate constants in both phases are not affected by partitioning. For cases where reactants or products are directly involved in phase separation, ideal behavior can no longer be assumed, and we refer to a recent article by Bauermann et al. who showed how chemical and phase equilibria are linked in such cases.[33]

We assume that all reactions can occur in both phases and that the reactants and products are transported between the phases. Partition coefficients ($\frac{k_{\mathrm{dil}\rightarrow\mathrm{cond}}}{k_{\mathrm{cond}\rightarrow\mathrm{dil}}} = \frac{c_{\mathrm{cond}}}{c_{\mathrm{dil}}} = K_{\mathrm{P}}$) are determined by the ratio of the transport rate from the dilute phase into the dense phase and the transport rate from the dense phase to the dilute phase, which is equal to the ratio of the concentration in the dense and dilute phase. We further assume for all systems studied in this paper that they are limited by the rate of the reactions and not by diffusion of reagents. This means that all species are evenly distributed in both phases at all times, and we do not consider spatial inhomogeneities or gradients within the dense or dilute phase. Since we focus here on condensates as protocellular microreactors and reactions relevant for the emergence of life, this assumption can easily be justified. Typical half-lives for prebiotic reactions in coacervates – including prebiotic TCA cycle reactions, oxidation reactions, template-directed replication and polymerization – are on the order of (half) hours to days[10,25,34] while typical diffusion rates inside coacervates are on the order of seconds to minutes, with experimental values measured at 10–100 $\mu m/s^2$ for smaller molecules,[35] and 0.1–10 for larger polymers such as RNA.[35,36] Given the 2–3 orders of magnitude difference in timescales of diffusion and reactions, all reactants can indeed be assumed to be evenly distributed, analogous to previous work on protein aggregation in two-phase systems by Weber et al., where the same assumption was made.[6,29] We note that this assumption greatly simplifies our model, as we do not take into account spatial coordinates in the dilute and dense phases, and thus, we do not consider effects such as active condensate size regulation or dynamic reaction-induced size instabilities that lead to division, which have been described by others.[37–39] Nevertheless, as we show below, even without spatial inhomogeneities, condensates can fundamentally affect the outcome of chemical reaction networks. Our model provides a convenient tool to better understand these effects for reactions that take place at timescales of tens of minutes to days, which covers most of prebiotic reactions and biological processes, including enzymatic reactions, RNA self-replication, protein aggregation and peptide synthesis.

In all simulations the ratio of volumes of the dilute phase to the dense phase is fixed and described by parameter $R = \frac{V_{\mathrm{dil}}}{V_{\mathrm{cond}}}$. For instance, $R = 100$ means that the volume of the dense phase is 100-times smaller than the volume of the dilute phase. We also note that the volume fraction of the dense phase ϕ is inversely related to R via $\phi = 1/(1+R)$.

All reactions and the transport equations compose a set of differential equations that are solved numerically to obtain the concentration of reactants over time (per phase). For example, for the first-order reaction ($A \rightarrow B$) we use the following set of equations:

$$\frac{d[A]_{\mathrm{dil}}}{dt} = k[A]_{\mathrm{dil}} - k_{\mathrm{dil}\rightarrow\mathrm{cond}}[A]_{\mathrm{dil}} + k_{\mathrm{cond}\rightarrow\mathrm{dil}}[A]_{\mathrm{cond}}$$

$$\frac{d[A]_{\mathrm{cond}}}{dt} = k[A]_{\mathrm{cond}} + Rk_{\mathrm{dil}\rightarrow\mathrm{cond}}[A]_{\mathrm{dil}} - Rk_{\mathrm{cond}\rightarrow\mathrm{dil}}[A]_{\mathrm{cond}}$$

where $[A]$ is the concentration of species A. The inclusion of R in the transport equation for the dense phase ensures that transporting one unit of concentration of reactant from the dilute phase to the dense phase produces R units of concentration in the dense phase (due to R-times smaller volume).

Systems of differential equations for more complex reactions are constructed analogously. Below we present the schematic representations of the reaction systems studied and we provide the full description of the corresponding systems of differential equations in Supplementary Information Section 1.

Rate Acceleration is Optimal for R = KP

To establish the foundations of chemical reaction kinetics in phase-separated droplets, we investigate a simple bimolecular reaction A + B → C in coacervates (Figure 1a), inspired by the aldol reactions and hydrazone formation reactions that have been reported in the presence of simple and complex coacervates.[10,11] Coacervates can influence reaction rates both by local accumulation of reactants and by changing the rate constant *k*due to the distinct local environment.[4] For reactants that are also involved in phase separation, Bauermann et al. recently showed that at phase equilibrium reaction rates for coacervate-forming (scaffold) molecules are solely determined by a change in *k*, because their chemical potential, and thus, activity is equal between the phases. However, this is different for the dilute guest molecules we consider here, as they do not contribute to phase separation. For dilute guests, the local concentration is therefore an important contributor to the reaction rate. This situation is reminiscent of the enhanced reactivity of hydrophobic compounds in micellar catalysis.[40] The effect of the local coacervate environment on reaction rates, is, however, difficult to generalize, because many factors – crowding, polarity, water activity, protonation equilibrium, and more – have non-trivial effects.[4] For example, interaction of reactants, transition states and products with the apolar or charged coacervate material can either accelerate or slow down a reaction, depending on the extent of (de)stabilization of the reactant, transition state and product of the reaction: if a

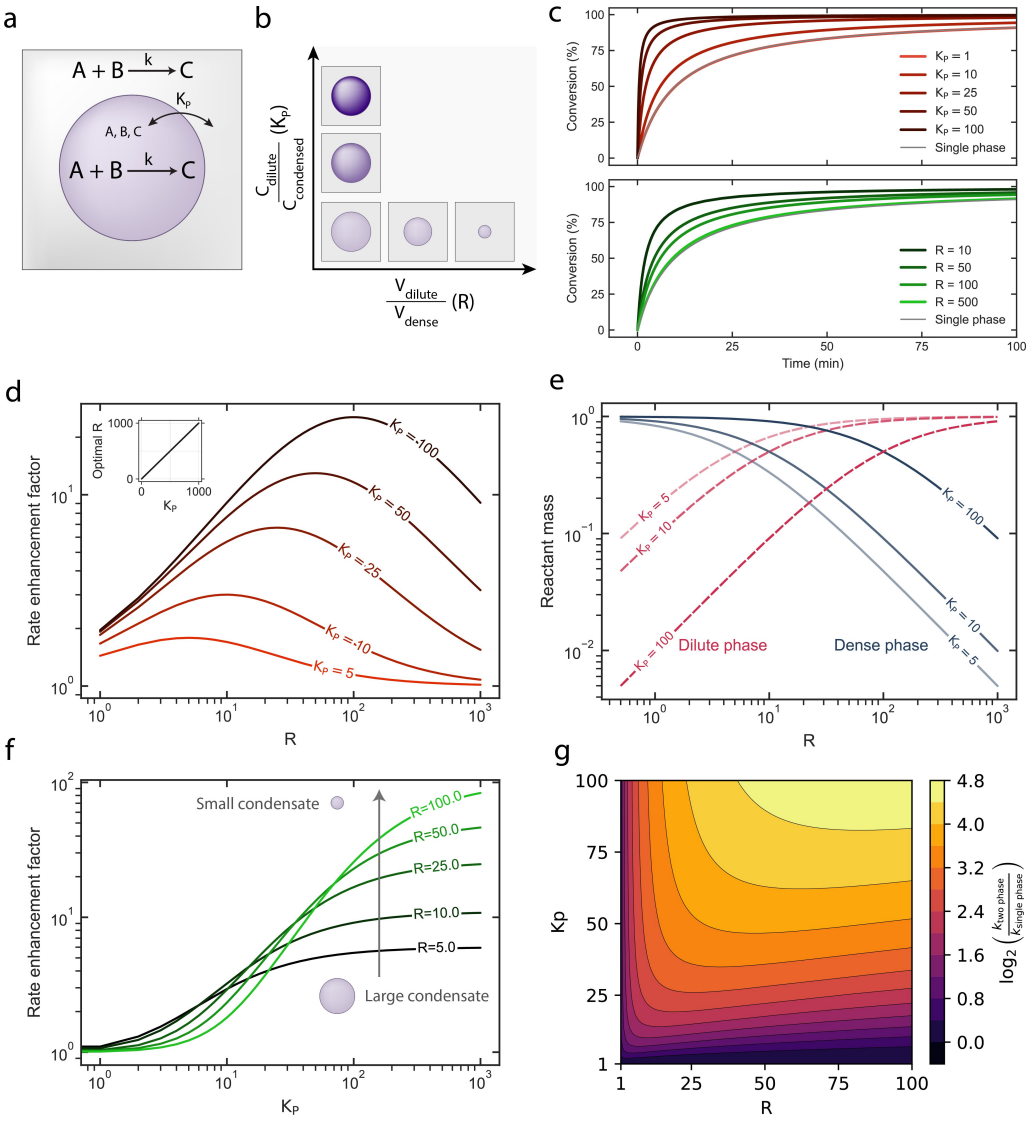

Figure 1. Bimolecular reaction system in two phases. (a) A bimolecular reaction A + B → C is modeled in two phases with an identical rate constant in both phases. All molecules can travel freely between both phases. (b) We vary the partition coefficient (K_P) and volume ratio (R) in our simulations. (c) Top: Higher partitioning of the components speeds up the reaction ($R = 100$). Bottom: Reaction rate converges to rate in single phase for very small coacervate volumes ($K_P = 10$). (d) For a set K_P, the relative rate enhancement ($k_{two\ phase}/k_{single\ phase}$) of the simple reaction in a two-phase system is optimal when R is equal to the K_P. Inset shows the R at which rate enhancement is maximum versus K_P. (e) At $R = K_P$ the dense and dilute phase contain an equal amount of reactant. An increase in R will lower the amount of reactant in the dense phase. (f) The rate enhancement of the reaction is always higher for a higher value of K_P, regardless of R. Larger compartments enhance the reaction more for smaller K_P, while smaller compartments have a larger increase for a higher K_P. (g) Heatmap of the overall rate enhancement for the full range of R and K_P.

reactant binds strongly to the coacervate material and is therefore stabilized, this may slow down the reaction, while stabilization of the product can accelerate it. These effects can effectively be captured in k, but are difficult to predict. Only a few experimental examples exist in literature where coacervate properties are directly linked to reaction kinetics.[9,11–13,17]

Therefore, we study the effect of concentration and changes in k here separately, and analyze the effect of local concentration on reaction kinetics in a two-phase system in this section first, and then discuss the influences of variations in the rate constants k. We vary K_P between 1–1000 and R between 1–1000 (i.e. from having 50% v/v to ~0.1% v/v dense phase), ranges that are achievable in experimental systems (Figure 1b). For simplicity, K_P's of all components are equal, unless otherwise specified. Experimental partition coefficients are often in the range of 2 to 50,[10,11,41] but values as high as $K_P =$ 10,000 have been reported.[42,43] The range of R in experimental systems can vary widely depending on the coacervate-forming components and the location in the phase diagram. For biomolecule-based coacervates, R is often in the range of 200–2000,[43] although R can become infinitely large at the edge of the phase diagram ($R \to \infty$ when $\phi \to 0$). On the other hand, for coacervates prepared with synthetic polymers (for which larger monomer concentrations can be obtained), values of R lower than 1 have been observed.[44]

First, we simulated how the partition coefficient K_P of the reactants affects the overall reaction time, with fixed $R = 100$. As expected, we find that higher partitioning leads to a faster reaction (Figure 1c). This simple example shows the potential of even relatively small amounts of coacervate phase to have a substantial effect on the overall reaction rate of the bulk. In the case of varying the phase volume ratio R (at fixed $K_P = 10$), we observe the highest rate enhancement for $R = 10$ with the reaction rate converging to the rate in a single phase for large values of R (Figure 1c), i.e. for a smaller volume of coacervate phase. This is to be expected, as for a smaller coacervate phase volume at constant partitioning, the relative contribution of the dense phase reaction to the overall reaction diminishes.

The observed rate enhancement by coacervates led us to investigate the relationship between R and K_P, by calculating the apparent overall rate constant based on the change in the total concentration of C ($k_{\text{two phase}}$). We normalized these apparent rate constants by dividing them by the rate constant of the single-phase reaction, given by rate constant $k_{\text{single phase}}$. We first analyzed how changing R at different, constant values of K_P changes the apparent rate constant of the entire system. We found that for any value of K_P there is an optimal value of R to achieve the highest rate enhancement (Figure 1d). Such a maximum was recently also observed by Laha et al.[31] Further analysis showed that the peak coincides with $R = K_P$, which we also find by analytically examining our system (Supplementary Information Section 2.1). This can be understood by considering that the optimal rate enhancement is related to the total amount of material within the coacervates and the local concentration. At $R = K_P$, the amount of reactant in the dense and dilute phase is equal (Figure 1e). Because the total amount of reactant is fixed, a decrease in R will result in a lower reactant concentration inside the dense phase (Supplementary Information Figure 3), and thereby lead to a lower local reaction rate inside the coacervates, while an increase in R will lower the amount of reactant in the dense phase (Figure 1e) and thereby reduce the effect of the dense phase reaction on the overall reaction rate. Further examination also showed that when the rate constant k is locally different inside the coacervate, the maximum rate enhancement is still approximately at $R = K_P$, even for a ten-fold increase in rate constant (Supplementary Information Section 2.1, Supplementary Figure 2).

On the other hand, when we varied K_P for a set of constant R values, we found that for any R, the highest rate can be achieved by increasing the K_P (Figure 1f). This observation can be rationalized by the fact that concentrating a larger number of molecules into a smaller compartment consistently results in a faster reaction. Interestingly, for smaller values of R rate enhancement is already observed for lower partitioning, but the maximum rate enhancement is limited due to the larger compartment. Smaller compartments show the potential to achieve higher overall rate enhancements, provided there is a sufficiently large K_P.

Taken together, these results highlight that rates are always highest when the reactants are concentrated as much as possible (i.e. high K_P), under the assumption that ideal solution behavior is retained, but for a given K_P, there is an optimal ratio of volumes for the two phases to achieve the highest rate enhancement (Figure 1g). We expect that in experimental and biological systems there is often partial control over the ratio of the two phases by controlling the concentration of the phase separating material, but there is limited control over the partitioning of the reactants. Although molecules could be functionalized with groups that enhance their partitioning, such modifications will often also affect their reactivity, especially in the case of small molecules. We show here that for such cases, tuning the volume ratio of the coacervate phase versus the dilute phase is a helpful method to control the reaction rate.

Coacervates Promote Longer Sequences in Polymerization Reactions

Inspired by these results for a simple bimolecular reaction, we wondered what effects coacervates could exert on more complex reactions and networks. We first investigated a polymerization reaction in coacervates. Studying the effect of coacervates on polymerization reactions can give important insights for the origins of life: the formation of the first biopolymers (RNA, DNA, peptides) is thought to be crucial for the emergence of life.[45,46] It is known that polymerization can be aided by minerals[47] or by drying the reaction mixture down to a paste,[48–50] as both these processes locally increase the concentration of reagents. Coacervates can similarly increase reagent concentration, but a systematic analysis of their effect on polymerization reactions is lacking.

To determine the effects of coacervates on the chain length and polydispersity of the polymerization products, we investigated a chain growth polymerization reaction (Figure 2a), in

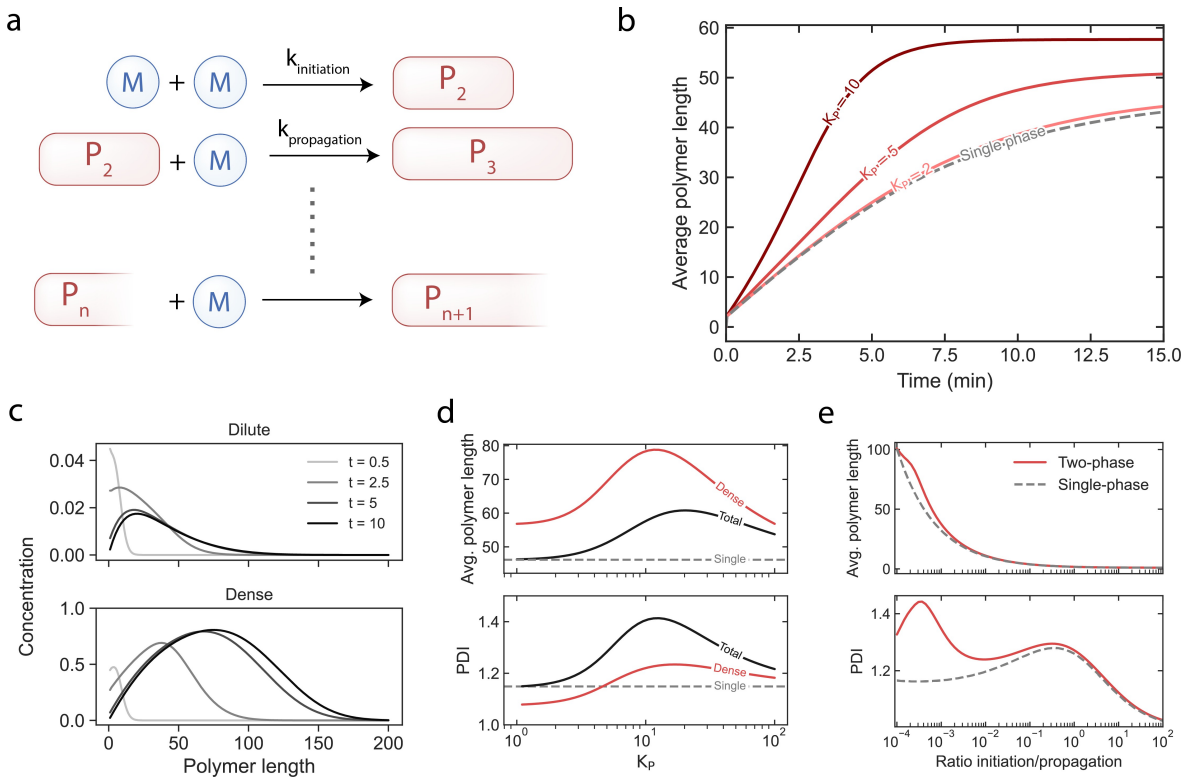

Figure 2. Polymerization in two phases. (a) Schematic overview of the chain growth polymerization reaction that can occur in two phases. Longer polymers have a lower transfer rate out of the coacervate, and therefore a higher K_P. (b) Increased partitioning leads to a faster formation of longer polymers and higher final average polymer length. K_P is defined as the K_P of the monomer ($R = 100$). (c) The dilute (top) and dense phase (bottom) have a distinct distribution of polymer lengths over the course of the reaction, with the dense phase retaining longer polymers ($K_{P,\ monomer} = 10$; $R = 100$). (d) Top: The number average final polymer length increases for stronger partitioning up to a maximum around $K_P = 20$ for the total sample and $K_P = 12$ for the dense phase. The final polymer length is consistently longer than for a single-phase system. Bottom: The obtained polydispersity index (PDI) follows a similar trend as the final average polymer length, with a maximum around KP = 10 for the total sample and $K_P = 15$ for the dense phase. (e) The obtained average polymer length and PDI vary as a function of the ratio of the initiation and propagation rate, with a pronounced difference between a single-phase and two-phase system for slow initiation compared to propagation ($K_{P,\ monomer} = 10$; $R = 100$).

which both the monomers and products partition into the coacervate. Because longer polymers have a stronger interaction with the coacervate matrix and have slower dynamics,[51,52] we modeled the longer polymers to have a lower $k_{cond\rightarrow dil}$ following an exponential decay and concomitant higher K_P (Supplementary Figure 6). We chose an exponential decay because according to Flory-Huggins theory the coacervate volume fraction φ_{coac} – and thus solubility – of long polymers scales approximately with $\varphi_{coac} = e^{-(\chi-1)N}$, with χ being the Flory-Huggins interaction parameter and N the degree of polymerization.[53] Even though long polymers are retained in one phase, the transfer of monomer should still be fast. We therefore expect the reaction rate to not become diffusion-limited even for high degrees of polymerization. We further assumed that all polymer lengths have equal $k_{propagation}$, and the polymerization to be living, i.e. to not terminate.

First, we modeled how the number average polymer length is affected by partitioning into coacervates compared to a single-phase reaction (Figure 2b, d). This was done by simulating the concentration of all polymeric species (up to a cutoff length n = 200). We confirmed that the cut-off length does not influence the output of our model: at the end of the reaction the concentrations of length 200 are below $1 \cdot 10^{-12}$ (Supplementary Figure 7–8, Supplementary Movie 1). We find that by increasing the partitioning of the reactants (K_P is the partition coefficient of the monomer), the reaction rate increases and long polymers are formed faster than in a single-phase reaction. Additionally, the final average polymer length is increased, up to a maximum for $K_P = 20$ (Figure 2d top). For $K_P > 20$ the average polymer length was found to decrease. Under these conditions, both the initiation and propagation take place almost exclusively in the dense phase (Supplementary Figure 9), and inside the dense phase the contribution of the initiation reaction increases (Supplementary Figure 10), most likely because of an increasingly high local concentration of monomers which has a comparatively larger effect on initiation (which is second-order in monomer) than on propagation (which is first-order in monomer). The maximum in polymer length as a function of K_P is directly related to the contributions of initiation and propagation to the total system, for which the minimum in contribution of initiation coincides with the maximum in average polymer length (Supplementary Figure 10). Changes in R also affect the average final polymer length, with larger R giving the largest final polymer length, while intermediate R gives a faster formation of long polymers (Supplementary Figure 12).

The increase in average polymer length is accompanied by a broadening of the distribution of polymer lengths (Supplementary Figure 8, Supplementary Movie 1), as the dense phase retains the long polymer sequences, while the dilute phase is enriched in shorter sequences (Figure 2c). This results in a higher polydispersity index (PDI) for moderate K_P's than for low K_P (Figure 2d bottom). For larger K_P's, however, the PDI decreases again following the decrease in average polymer length. The polydispersity in a single-phase system is, however, always lower than in a two-phase system. Nevertheless, for low to intermediate K_P the local PDI of all polymers in the dense phase is lower than the PDI of all polymers formed in a single-phase system, while a higher average polymer length is obtained. This suggests that coacervates may serve to select polymers based on length, and reduce the local variations in length. Isolation of the dense phase after the polymerization reaction is completed may yield long polymers with a low polydispersity.

To generalize our model for polymerization reactions with different rates, we modulated the ratio between the rate of initiation and propagation. We analyzed the average polymer length at the end of the reaction (Figure 2e) for both a two-phase and a single-phase system. Only for slow initiation compared to propagation (low ratio) a difference is observed between a two-phase and single-phase system, with the reaction in a two-phase system leading to a larger final polymer length. For faster initiation, more polymers are nucleated and the final polymer length is shorter due to the limited amount of monomer. Under these conditions, coacervates do not make a significant difference to the final polymer length that is obtained, because, due the shorter final length, the effect of retention of longer sequences in the coacervate is less strong. Also, the difference in PDI is larger for slow initiation and diminishes for fast initiation, although for the PDI the difference between a two-phase and single-phase system remains up to higher ratios of initiation to propagation.

These results show that coacervates are a promising environment for forming longer polymers. Isolation of the dense phase after completion of the reaction could yield long polymers with low PDI and might be useful for industrial purposes. For the origins of life, we would argue that the importance of forming longer sequences outweighs the disadvantage of having a larger PDI in the total two-phase system. The formation of longer polymers would make it possible to store more information in the first genetic polymers and these longer sequences could be selectively retained inside coacervate protocells. Longer sequences of RNA are also more likely to gain catalytic function. Similarly, longer peptide sequences are more likely to have a defined fold or undergo phase separation, which would allow the coacervate to promote the formation of its own material. Lastly, a larger population of long polymers can cover a larger sequence space, increasing the chance of creating functional sequences.

Self-Replication Rate can be Increased in Coacervates

To replicate the sequence information stored in prebiotic biopolymers, self-replication is thought to have preceded more complex enzyme-based replication.[54,55] Self-replicating DNAs,[56,57] peptides,[58,59] ribozymes[60–62] and synthetic molecules[63,64] have been developed, which replicate themselves by coordination of two building blocks to a template, which increases the effective molarity of the building blocks and facilitates their ligation, forming a copy of the template molecule (Figure 3a). A general problem in most of these systems, however, is product inhibition: dissociation of the formed template duplex is so slow that it prevents the product template from catalyzing a new round of replication.[54] Coacervates have been shown to melt nucleic acid duplexes,[65,66] and could therefore potentially alleviate product inhibition. This is a delicate balance, as the same interactions that weaken the template duplex are also likely to weaken the interaction between template and building blocks.[3] Another step in the replication process that coacervates can affect is the rate of ligation between the building blocks, which can be increased due to a higher local concentration.

The functioning of self-replicators inside coacervate protocells has recently received a lot of attention. Several self-replicating DNA and ribozyme systems have been shown to function inside coacervates,[23,34,67] and in some cases the replication rate is even enhanced.[14] How well self-replication works is highly dependent on the nature of the coacervate material.[34,67] We aimed to get a deeper understanding of how coacervates can promote self-replication and help overcome product inhibition.

We modeled a templated self-replication reaction with two pathways, a non-catalytic pathway in which a bimolecular reaction of A + B forms template T, and a catalytic pathway in which A and B coordinate to T to form a complex [ABT] upon which ligation forms a duplex of templates TT, which are subsequently released (Figure 3a). We assessed if the introduction of the coacervate phase could change the relation of the autocatalytic pathway to the non-autocatalytic pathway. To do so, we integrate the total concentration of T formed through both reactions over time (Figure 3b). For visualization purposes, system parameters were chosen so that cumulative contributions of both reactions are close to equal in the single-phase system, starting with no T present. Under these conditions $\frac{k_{\text{autocatalytic ligation}}}{k_{\text{bimolecular}}} = 16.4$, which is in the lower range of values found for experimental self-replicating systems (Supplementary Table 5).[57,58,60,68] The results for a 100x larger ratio between the pathways are similar and are described in Supplementary Information Section 4.3. We normalize the total contribution of both pathways to 1 to compare how the relative contributions of both reactions change in a two-phase system with differing K_P of the components (Figure 3c). We assumed that all reaction components partition to the same extent.

In the case of equal partitioning between the coacervate and coexisting dilute phase ($K_P = 1$), no change in the relative contributions is found compared to a single-phase system, as expected. However, we find that beyond $K_P = 1$, there is an

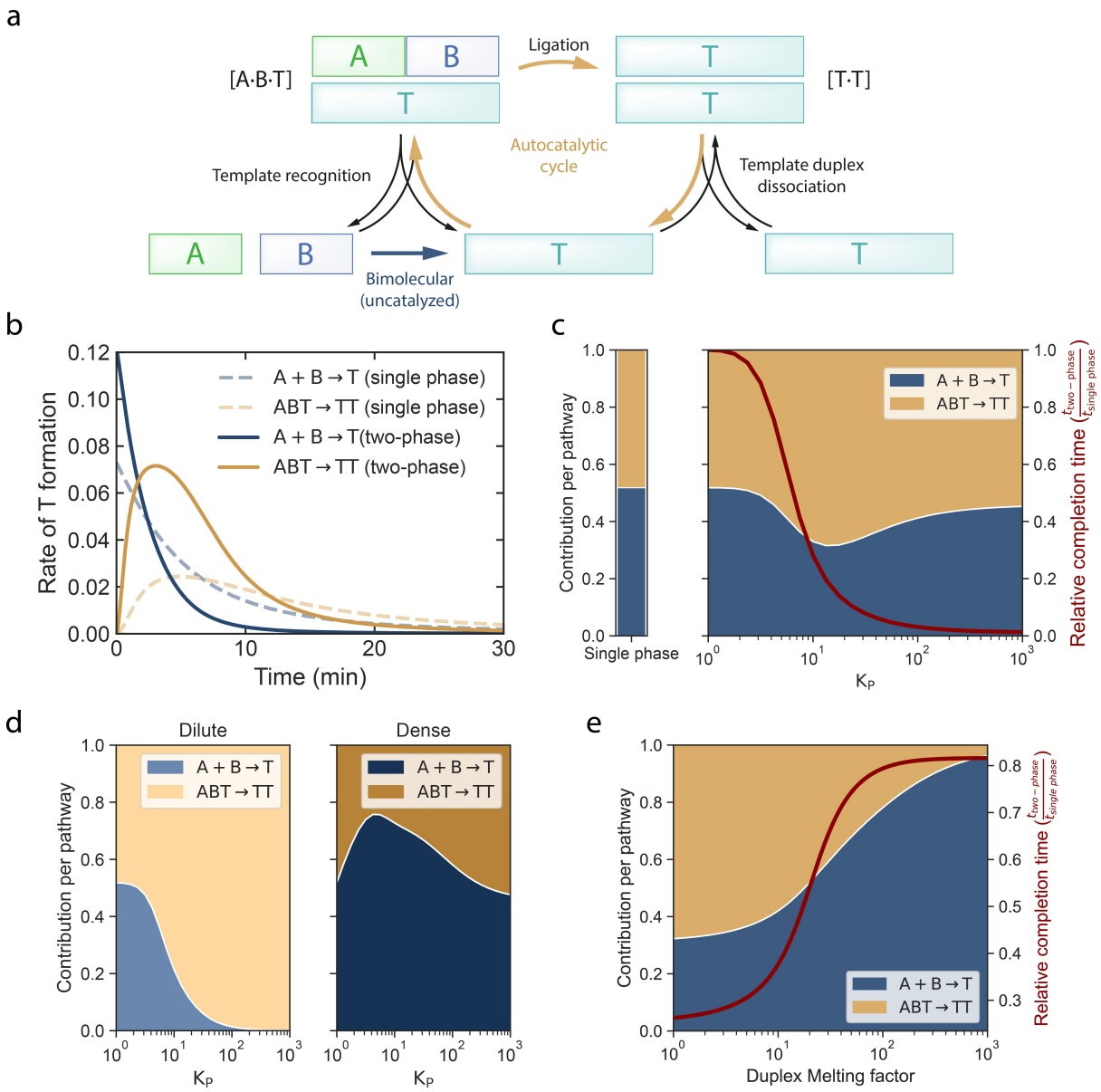

Figure 3. Self-replication in two phases. (a) Schematic overview of the self-replication that can take place in a two-phase system. Building blocks A and B can react in an uncatalyzed bimolecular reaction to form template T, which can then catalyze its own formation by binding the building blocks and aiding their ligation. A common limitation in most experimental systems is the slow dissociation of the template duplex to release the template strands for a further round of replication. (b) A comparison between the T formed through the autocatalytic (ABT → TT) and non-autocatalytic pathway (A + B → T) in a single phase and in a two-phase system ($K_P = 10$, $R = 100$). (c) The contribution of the autocatalytic pathway has a maximum around $K_P = 10$, after which it decreases again for large K_P. The completion time for the reaction (normalized to the completion time in a single-phase system) decreases as a function of K_P. K_P is kept equal for all components in the system. (d) In the dilute phase, an increased K_P leads to nearly exclusively autocatalytic formation of T. In the dense phase, the non-autocatalytic pathway reaches a maximum around $K_P = 5$, after which it decreases to an equal contribution of both pathways at large K_P. (e) Duplex melting within the dense phase leads to an increase in the non-autocatalytic pathway, while increasing the completion time for the reaction ($K_P = 10$, $R = 100$).

optimum in the relative contribution of the autocatalytic reaction to the self-replication at intermediate K_P. For higher partitioning the formation of T occurs faster, while the contribution of the autocatalytic pathway decreases again (Figure 3c). When we divide the contributions between the two phases, we can see that in the dilute phase the reaction is increasingly autocatalytic for higher K_P (Figure 3d). The dense phase, on the other hand, starts with equal contribution of both pathways for $K_P = 1$, but shows a strong increase in contribution from the bimolecular pathway until a maximum is reached at $K_P = 5$, after which its contribution decreases again. For low K_P (up to $K_P = 10$) the reaction in the dilute phase has the largest effect on the overall distribution of pathways in Figure 3c. However, for larger K_P ($K_P > 30$), the reaction in the dense phase starts to determine the overall reactions (Supplementary Figure 15), as under these conditions the majority of the reactant mass is in the dense phase and the majority of T is formed there. By inhibiting transfer between the phases for

individual components (Supplementary Figure 16–22), we were able to find that transfer of ABT from the dense to the dilute phase is critical to obtain the contributions in Figure 3c. Formation of ABT is the most unfavorable step, as it is the step with the highest molecularity. The high concentration in the dense phase favors ABT formation (Supplementary Figure 23–24), after which it is rapidly transferred to the dilute phase, where it reacts to form TT (Supplementary Figure 25). These observations show that free transfer between the phases is crucial for the functioning of the self-replication reaction in a two-phase system. Although a concentration-dependent distribution of the pathways is also observed in a single phase (Supplementary Figure 14), the maximum contribution of the autocatalytic pathway is slightly larger in the two-phase system (0.3 vs. 0.4), and, most importantly, the completion time for the reaction can be significantly reduced in a two-phase system (Figure 3c), without having to increase the overall reagent concentration.

To investigate the effect of coacervates on product inhibition, we modulated the strength of complex formation between $T + T \leftrightarrow TT$ and $A + B + T \leftrightarrow ABT$ by introducing a 'duplex melting factor' that increases the dissociation constant for both equilibria to the same extent. In experimental systems, such an increase in dissociation constant could be obtained by changing the charge-density, charge-type, length and charge-balance of the coacervate components,[22,34,67,69] or by the extent of Mg^{2+} partitioning for ribozyme self-replicators.[67] Increasing the duplex melting factor increases the contribution of the bimolecular pathway (Figure 3e), and increases the relative completion time. It is therefore unlikely that coacervates will alleviate product inhibition, especially considering that in experimental systems the termolecular ABT complex is likely weakened more than the bimolecular TT complex.

Although reduction of product inhibition cannot be achieved with coacervates – and must instead be achieved by structurally changing the reactants or by temporal changes in the dissociation constant – coacervates can aid self-replication reactions by accelerating the reaction through local accumulation of reagents, making it more likely for self-replication to take place in the dilute conditions on prebiotic Earth.

Coacervates can Alter the Periodicity and Robustness of Oscillating Chemical Reaction Networks

Lastly, we investigated how coacervates can affect more complex reaction networks, such as networks that display oscillatory behavior. Oscillatory behavior can emerge in out-of-equilibrium systems and is known to drive many processes important to life, such as circadian rhythm and the cell-cycle.[70,71] Oscillations can only be achieved when a chemical network system is complex enough and there is sufficient delay in the reactions.[72,73] The periodicity, amplitude and persistence of oscillations are dependent on reactant concentrations and rate constants, and could therefore be tuned by the local conditions inside the coacervate phase.

We modeled an oscillating system based on the Brusselator[74–76] (Figure 4a) to investigate what effect K_P, R and the transfer rate between the phases can have on oscillations. We started with varying K_P and observe that stronger partitioning results in a shorter period and lower amplitude of the oscillations (Figure 4b, e, Supplementary Figure 31, Supplementary Movie 2). To determine the period of the oscillations, we found local maxima by comparing neighboring values and calculated the average time between them for oscillations between 5 and 50 minutes. Around $K_P = 11$, the limit cycle breaks down and the oscillation becomes unstable (Supplementary Movie 2). Similar behavior is observed for a single-phase system at high concentrations (Supplementary Figure 32–33). In addition to K_P, the period and amplitude are also affected by R(Figure 4c–e, Supplementary Figure 31, Supplementary Movie 3). The period does not decrease linearly upon R, but has a steep decline between $R = 25$ and $R = 35$, after which it reaches a minimum around $R = 40$ and it slowly increases again for larger R. The onset of the steep decline corresponds to the point where the oscillations collapse into a smaller limit cycle and the system undergoes transient instability before entering the limit cycle (Figure 4d, Supplementary Figure 34–35, Supplementary Movie 3). The maximum amplitude, however, does show a gradual decrease for larger R, but similarly increases again for large R.

In addition to giving changes in amplitude and periodicity of oscillations, coacervates can help to sustain oscillations in concentration regimes that do not give sustained oscillations in a single phase because they do not fulfill the criterion $[B] < [A]^2 + 1$ (Figure 4e top). When B partitions more strongly than A – in this case $K_{P\,A,C,X,Y} = 5$ and $K_{P\,B} = 30$ – the concentrations inside the coacervate phase still obey the criterion for sustained oscillations, and stable oscillations are maintained in the system overall. In this way, coacervates can increase the robustness of the oscillatory network.

The changes in period, amplitude and robustness caused by including oscillatory reaction networks in a two-phase system affect the timekeeping and output of the system, and thereby alter its function. Such changes can have profound effects on downstream reactions coupled to the oscillatory network,[77] and could possibly play a role in oscillating biomolecular reaction networks in the cell in the presence of biocondensates.

Conclusions

In this work, we have shown that coacervates can direct outcomes of several chemical reaction systems. We found that the reaction rate of elementary bimolecular reactions can be significantly increased in coacervates and can be optimized by either increasing the partition coefficient, or by adjusting the phase volume ratio R to equal K_P. These insights allow for optimization of reactions rates in experimental systems by either modifying the reactants to have stronger partitioning or by adjusting the amount of coacervate material to get the desired volume ratio. We further showed that coacervates can cause unexpected outcomes for more complex reactions. For

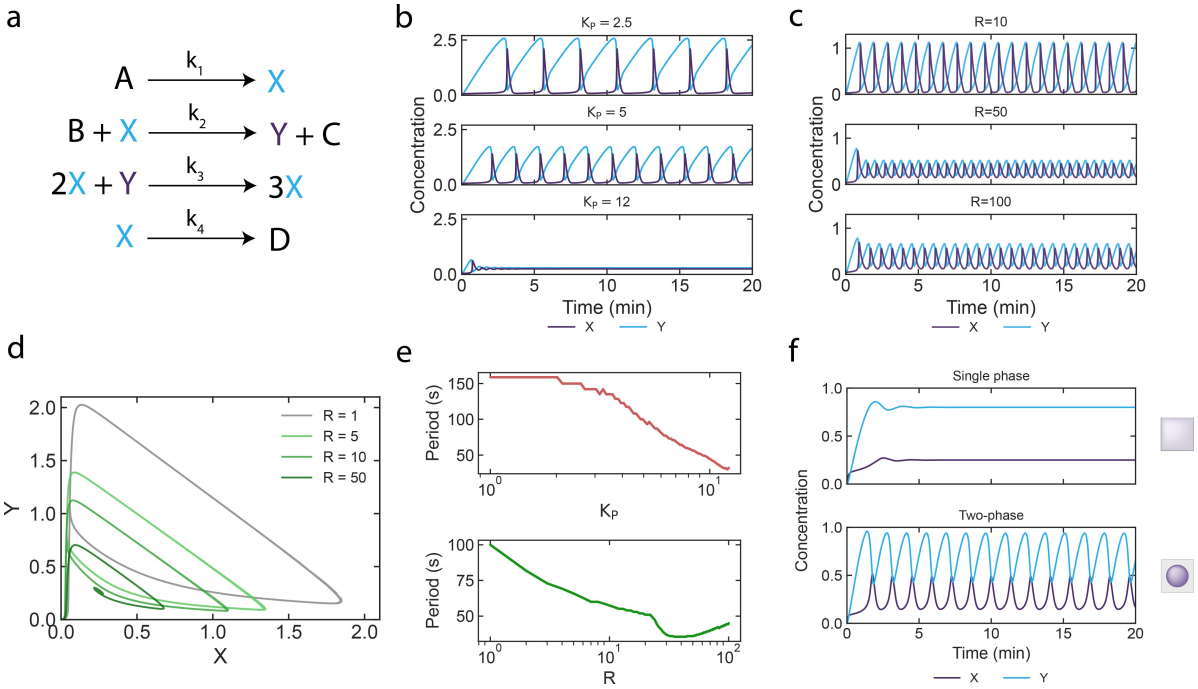

Figure 4. Oscillatory reactions in two phases. (a) Schematic overview of the Brusselator reactions. All reaction components partition equally into the coacervate phase. (b) A larger K_P lowers the periodicity and amplitude of the oscillations ($R = 100$). At $K_P = 12$ sustained oscillations are no longer observed. (c) A larger R lowers the periodicity and amplitude of the oscillations down to a minimum, after which they increase again. (d) Phase plot showing the decreased periodicity and amplitude for higher R ($K_P = 10$). At $R = 50$, the system undergoes transient instability before entering the limit cycle. (e) Average period of oscillations between 5 and 50 minutes of the reaction as a function of K_P ($R = 100$) and R ($K_P = 10$). The period decreases as a function of K_P up to $K_P = 11$. The period of oscillations decreases as a function of R with an increase in slope around $R = 25$, and a minimum around $R = 40$, after which the period increases again. (f) For different partitioning of reactants, a two-phase system (bottom; $K_{P\,A,C,X,Y} = 5$, $K_{P\,B} = 30$, $R = 100$) can sustain oscillations at overall concentrations that do not give sustained oscillations in a single phase (top).

polymerization reactions, inclusion in coacervates can lead to faster polymerization and formation of longer polymers. For self-replication, the reaction can be significantly accelerated by introduction into a two-phase system, although duplex melting inside the coacervate does not help to alleviate product inhibition. Lastly, coacervates can affect both the periodicity and amplitude of oscillating networks and can even 'rescue' oscillations in concentration regimes where oscillations are not sustained in a single-phase system.

We modeled a simple example of a self-replicator and oscillating network. Experimental examples of such nonlinear systems are inherently more complex and can have complex dependencies on factors such as temperature or reagent concentration, even in a single phase system. To model the effect of coacervates on a specific experimental system, these dependencies would therefore have to be taken into account, and may result in a different outcome. Our model does, however, provide an example of the effect that a two-phase system can have on nonlinear systems such as self-replicators and oscillating networks.

In our model we assumed transfer between the phases to be non-limiting (except for the polymerization reaction), so that a single large coacervate droplet is equivalent to several small droplets. In some experimental systems, however, the interface might form a physical barrier for transport between the coacervate phase and the dilute phase due to the interfacial resistance.[78] This effect is expected to be stronger for larger molecules that can adopt different conformations, of which some do not interact with the coacervate material due to shielding of interacting regions of the sequence, and would therefore 'bounce off' the interface. In such cases a large coacervate surface area (as is obtained for many small droplets) would slow down exchange and a single large coacervate droplet would be more favorable. In the case of diffusion-limited reactions, however, a large interface area might actually be advantageous, as under these conditions substrate can be supplemented from the dilute phase more rapidly. For such cases, the coacervate surface area (and therefore droplet size) will further influence the kinetics of the system, and may give rise to emergent phenomena such as synchronization.

Taken together, our results show that coacervates hold great promise as microreactors that could direct the outcome of a wide range of reactions, including biochemical reactions in biological condensates, prebiotic reactions at the origins of life and synthetic reactions for industrial purposes.

Supporting Information

Additional simulation results, methods, rate equations and model parameters, analytical derivation of the relationship

between R and K_P for bimolecular reactions, supplementary movies of phase plots and polymer length distribution (PDF).

Acknowledgments

This project received funding from the European Research Council (ERC) under the European Union's Horizon 2020 research and innovation program under grant agreement number 851963, and a Vidi grant from the Netherlands Organization for Scientific Research (NWO).

Conflict of Interests

The authors declare no conflict of interest.

Data Availability Statement

Data sharing is not applicable to this article as no new data were created or analyzed in this study.

Keywords: biocondensates · coacervate protocells · compartmentalization · reaction kinetics · catalysis

[1] N. A. Yewdall, A. A. M. André, T. Lu, E. Spruijt, *Curr. Opin. Colloid Interface Sci.* **2021**, *52*, 101416.
[2] B. Ghosh, R. Bose, T. Y. D. Tang, *Curr. Opin. Colloid Interface Sci.* **2021**, *52*, 101415.
[3] A. D. Slootbeek, M. H. I. van Haren, I. B. A. Smokers, E. Spruijt, *Chem. Commun.* **2022**, *58*, 11183–11200.
[4] I. B. A. Smokers, B. S. Visser, A. D. Slootbeek, W. T. S. Huck, E. Spruijt, *Acc. Chem. Res.* **2024**, *15*, 39.
[5] S. F. Banani, H. O. Lee, A. A. Hyman, M. K. Rosen, *Nat. Rev. Mol. Cell Biol.* **2017**, *18*, 285–298.
[6] W. P. Lipiński, B. S. Visser, I. Robu, M. A. A. Fakhree, S. Lindhoud, M. M. A. E. Claessens, E. Spruijt, *Sci. Adv.* **2022**, *8*, 6495.
[7] C. Mathieu, R. V. Pappu, J. Paul Taylor, *Science* **2020**, *370*, DOI 10.1126/science.abb8032.
[8] M. H. I. Van Haren, K. K. Nakashima, E. Spruijt, *J. Syst. Chem.* **2020**, *8*, 107–120.
[9] S. Koga, D. S. Williams, A. W. Perriman, S. Mann, *Nat. Chem.* **2011**, *3*, 720–724.
[10] I. B. A. Smokers, M. H. I. van Haren, T. Lu, E. Spruijt, *ChemSystemsChem* **2022**, *4*, e202200004.
[11] M. Abbas, W. P. Lipiński, K. K. Nakashima, W. T. S. Huck, E. Spruijt, *Nat. Chem.* **2021**, *13*, 1046–1054.
[12] M. I. Jacobs, E. R. Jira, C. M. Schroeder, *Langmuir* **2021**, *37*, 14323–14335.
[13] W. Peeples, M. K. Rosen, *Nat. Chem. Biol.* **2021**, *17*, 693–702.
[14] S. Ameta, M. Kumar, N. Chakraborty, Y. J. Matsubara, S. Prashanth, D. Gandavadi, S. Thutupalli, *Commun. Chem.* **2023**, *6*, 1–10.
[15] B. Saha, A. Chatterjee, A. Reja, D. Das, *Chem. Commun.* **2019**, *55*, 14194–14197.
[16] J. Crosby, T. Treadwell, M. Hammerton, K. Vasilakis, M. P. Crump, D. S. Williams, S. Mann, *Chem. Commun.* **2012**, *48*, 11832–11834.
[17] A. M. Küffner, M. Prodan, R. Zuccarini, U. Capasso Palmiero, L. Faltova, P. Arosio, *ChemSystemsChem* **2020**, *2*, e2000001.
[18] K. K. Nakashima, M. A. Vibhute, E. Spruijt, *Front. Mol. Biosci.* **2019**, *6*, 21.
[19] W. Mu, Z. Ji, M. Zhou, J. Wu, Y. Lin, Y. Qiao, *Sci. Adv.* **2021**, *7*, 9000–9028.
[20] K. Lv, A. W. Perriman, S. Mann, *Chem. Commun.* **2015**, *51*, 8600–8602.
[21] R. R. Poudyal, C. D. Keating, P. C. Bevilacqua, *ACS Chem. Biol.* **2019**, *14*, 1243–1248.
[22] K. Le Vay, E. Y. Song, B. Ghosh, T. Y. D. Tang, H. Mutschler, *Angew. Chem. Int. Ed.* **2021**, *60*, 26096–26104.
[23] K. K. Le Vay, E. Salibi, B. Ghosh, T. Y. Dora Tang, H. Mutschler, *eLife* **2023**, *12*, DOI 10.7554/eLife.83543.
[24] W. A. Wee, H. Sugiyama, S. Park, *iScience* **2021**, *24*, 103455.
[25] J. Wang, M. Abbas, J. Wang, E. Spruijt, *Nat. Commun.* **2023**, *14*, 1–11.
[26] R. R. Poudyal, R. M. Guth-Metzler, A. J. Veenis, E. A. Frankel, C. D. Keating, P. C. Bevilacqua, *Nat. Commun.* **2019**, *10*, 1–13.
[27] T. P. Fraccia, N. Martin, *Nat. Commun.* **2023**, *14*, 1–12.
[28] E. Sokolova, E. Spruijt, M. M. K. Hansen, E. Dubuc, J. Groen, V. Chokkalingam, A. Piruska, H. A. Heus, W. T. S. Huck, *Proc. Natl. Acad. Sci. USA* **2013**, *110*, 11692–11697.
[29] C. Weber, T. Michaels, L. Mahadevan, *eLife* **2019**, *8*, DOI 10.7554/eLife.42315.
[30] T. C. T. Michaels, L. Mahadevan, C. A. Weber, *Phys. Rev. Res.* **2022**, *4*, 043173.
[31] S. Laha, J. Bauermann, F. Jülicher, T. C. T. Michaels, C. A. Weber, *arXiv* **2024**, *2403.05228*, DOI 10.48550/arXiv.2403.05228.
[32] W. Fan, *bioRxiv* **2023**, 2023.11.04.565634.
[33] J. Bauermann, S. Laha, P. M. McCall, F. Jülicher, C. A. Weber, *J. Am. Chem. Soc.* **2022**, *144*, 19294–19304.
[34] R. R. Poudyal, R. M. Guth-Metzler, A. J. Veenis, E. A. Frankel, C. D. Keating, P. C. Bevilacqua, *Nat. Commun.* **2019**, *10*, 1–13.
[35] R. B. Lira, J. Willersinn, B. V. K. J. Schmidt, R. Dimova, *Macromolecules* **2020**, *53*, 10179–10188.
[36] K. Rhine, S. Skanchy, S. Myong, *Methods* **2022**, *197*, 74–81.
[37] C. A. Weber, D. Zwicker, F. Jülicher, C. F. Lee, *Rep. Prog. Phys.* **2019**, *82*, 064601.
[38] J. Kirschbaum, D. Zwicker, *J. R. Soc. Interface* **2021**, DOI 10.1098/RSIF.2021.0255.
[39] D. Zwicker, R. Seyboldt, C. A. Weber, A. A. Hyman, F. Jülicher, *Nat. Phys.* **2017**, *13*, 408–413.
[40] S. Mattiello, E. Ghiglietti, A. Zucchi, L. Beverina, *Curr. Opin. Colloid Interface Sci.* **2023**, *64*, 101681.
[41] J. G. Dumelie, Q. Chen, D. Miller, N. Attarwala, S. S. Gross, S. R. Jaffrey, *Nat. Chem. Biol.* **2024**, *20*, 302–313.
[42] S. A. Thody, H. D. Clements, H. Baniasadi, A. S. Lyon, M. S. Sigman, M. K. Rosen, *Nat. Chem.* **2024** .
[43] E. A. Frankel, P. C. Bevilacqua, C. D. Keating, *Langmuir* **2016**, *32*, 2041–2049.
[44] Q. Wang, J. B. Schlenoff, *Macromolecules* **2014**, *47*, 3108–3116.
[45] P. Canavelli, S. Islam, M. W. Powner, *Nature* **2019**, *571*, 546–549.
[46] F. Müller, L. Escobar, F. Xu, E. Węgrzyn, M. Nainytė, T. Amatov, C. Y. Chan, A. Pichler, T. Carell, *Nature* **2022**, *605*, 279–284.
[47] R. Liu, L. E. Orgel, *Origins Life Evol. Biospheres* **1998**, *28*, 245–257.
[48] M. Frenkel-Pinter, J. W. Haynes, A. M. Mohyeldin, C. Martin, A. B. Sargon, A. S. Petrov, R. Krishnamurthy, N. V. Hud, L. D. Williams, L. J. Leman, *Nat. Commun.* **2020**, *11*, 1–14.
[49] M. Frenkel-Pinter, M. Bouza, F. M. Fernández, L. J. Leman, L. D. Williams, N. V. Hud, A. Guzman-Martinez, *Nat. Commun.* **2022**, *13*, 1–8.
[50] M. Frenkel-Pinter, J. W. Haynes, C. Martin, A. S. Petrov, B. T. Burcar, R. Krishnamurthy, N. V. Hud, L. J. Leman, L. D. Williams, *Proc. Natl. Acad. Sci. USA* **2019**, *116*, 16338–16346.
[51] K. Kamagata, N. Iwaki, S. Kanbayashi, T. Banerjee, R. Chiba, V. Gaudon, B. Castaing, S. Sakomoto, *Sci. Rep.* **2022**, *12*, 1–11.
[52] S. Coupe, N. Fakhri, *Biophys. J.* **2023**, DOI 10.1016/j.bpj.2023.07.013.
[53] S. H. M. van Leuken, R. A. T. M. van Benthem, R. Tuinier, M. Vis, *Macromol. Theory Simul.* **2023**, *32*, DOI 10.1002/MATS.202300001.
[54] H. Duim, S. Otto, *Beilstein J. Org. Chem.* **2017**, *13*, 1189–1203.
[55] K. Le Vay, L. I. Weise, K. Libicher, J. Mascarenhas, H. Mutschler, *Adv. Biosyst.* **2019**, *3*, 1800313.
[56] W. S. Zielinski, L. E. Orgel, *Nature* **1987**, *327*, 346–347.
[57] G. von Kiedrowski, *Angew. Chem. Int. Ed. Engl.* **1986**, *25*, 932–935.
[58] D. H. Lee, J. R. Granja, J. A. Martinez, K. Severin, M. R. Ghadiri, *Nature* **1996**, *382*, 525–528.
[59] B. Rubinov, N. Wagner, H. Rapaport, G. Ashkenasy, *Angew. Chem. Int. Ed.* **2009**, *48*, 6683–6686.
[60] N. Paul, G. F. Joyce, *Proc. Natl. Acad. Sci. USA* **2002**, *99*, 12733–12740.
[61] T. A. Lincoln, G. F. Joyce, *Science* **2009**, *323*, 1229–1232.
[62] N. Vaidya, M. L. Manapat, I. A. Chen, R. Xulvi-Brunet, E. J. Hayden, N. Lehman, *Nature* **2012**, *491*, 72–77.
[63] J. M. A. Carnall, C. A. Waudby, A. M. Belenguer, M. C. A. Stuart, J. J. P. Peyralans, S. Otto, *Science* **2010**, *327*, 1502–1506.
[64] T. Tjivikua, P. Ballester, J. Rebek, *J. Am. Chem. Soc.* **1990**, *112*, 1249–1250.
[65] T. J. Nott, T. D. Craggs, A. J. Baldwin, *Nat. Chem.* **2016**, *8*, 569–575.
[66] F. P. Cakmak, S. Choi, M. C. O. Meyer, P. C. Bevilacqua, C. D. Keating, *Nat. Commun.* **2020**, *11*, DOI 10.1038/s41467-020-19775-w.

[67] J. M. Iglesias-Artola, B. Drobot, M. Kar, A. W. Fritsch, H. Mutschler, T. Y. Dora Tang, M. Kreysing, *Nat. Chem.* **2022**, *14*, 407–416.
[68] R. Issac, J. Chmielewski, *J. Am. Chem. Soc.* **2002**, *124*, 6808–6809.
[69] F. P. Cakmak, S. Choi, M. C. O. Meyer, P. C. Bevilacqua, C. D. Keating, *Nat. Commun.* **2020**, *11*, DOI 10.1038/s41467-020-19775-w.
[70] J. C. Dunlap, *Cell* **1999**, *96*, 271–290.
[71] A. Goldbeter, M. J. Berridge, *Biochemical Oscillations and Cellular Rhythms*, Cambridge University Press, **1996**.
[72] B. Novák, J. J. Tyson, *Nat. Rev. Mol. Cell Biol.* **2008**, *9*, 981–991.
[73] S. N. Semenov, A. S. Y. Wong, R. M. Van Der Made, S. G. J. Postma, J. Groen, H. W. H. Van Roekel, T. F. A. De Greef, W. T. S. Huck, *Nat. Chem.* **2015**, *7*, 160–165.
[74] I. Prigogine, R. Lefever, *J. Chem. Phys.* **1968**, *48*, 1695–1700.
[75] R. Yoshida, *Adv. Mater.* **2010**, *22*, 3463–3483.
[76] V. K. Vanag, I. R. Epstein, *Phys. Rev. Lett.* **2001**, *87*, 228301–228301-4.
[77] M. ter Harmsel, O. R. Maguire, S. A. Runikhina, A. S. Y. Wong, W. T. S. Huck, S. R. Harutyunyan, *Nature* **2023**, *621*, 87–93.
[78] Y. Jiang, A. Pyo, C. P. Brangwynne, H. A. Stone, N. S. Wingreen, Y. Zhang, *Biophys. J.* **2023**, *122*, 442a.

Manuscript received: July 12, 2024
Accepted manuscript online: August 21, 2024
Version of record online: October 29, 2024